

# The role of singularity points in the dynamics of a chemostat

CAMMAROTA Andrea  
[acammarota@unisa.it](mailto:acammarota@unisa.it)

MICCIO Michele  
[mmiccio@unisa.it](mailto:mmiccio@unisa.it)

POLETTA Massimo  
[mpoletto@unisa.it](mailto:mpoletto@unisa.it)

Dipartimento di Ingegneria Chimica ed Alimentare, Università di Salerno  
Via Ponte don Melillo - 84084 FISCIANO SA  
Italy

In this work the dynamic behavior of a chemostat has been theoretically studied with the support of the singularity theory. The bioreactor is described by a simple two-dimensional, unstructured ODE model accounting for biomass and controlling substrate mass balances with variable yield coefficient. The main aim is an in-depth investigation on the dynamics of the bioreactor, in particular on the presence and the role of codimension one singularities. In comparison with the previous work of Ajbar (2001), a more extensive analysis has been performed and the role of all the involved parameters is evaluated. In particular, the effects of kinetic parameters and yield variability on the dynamics of the bioreactor are systematically investigated. Therefore, for this system, an exhaustive non-persistent bifurcation diagram is drawn; it allows exploiting the conditions that determine dynamic regimes in the bioreactor and, to some extent, their stability features.

## 1 Introduction.

The chemostat is a continuous bioreactor for microbial cultivation operating at a constant reaction volume and characterised by a constant inlet flow rate of constant composition (Bailey & Ollis, 1986). It is, probably, the simplest and the most widespread type of continuous bioreactor. Its dimensionless mass balance equations can be expressed in the following form:

$$\begin{cases} x'(t) = [\mu(s(t)) - dil - k_d]x(t) \\ s'(t) = dil(1 - s(t)) - \frac{\mu(s(t))}{y(s(t))}x(t) \end{cases} \quad (1.)$$

where  $x$  is the biomass concentration,  $s$  the limiting substrate concentration and  $dil$  the dilution rate. The adopted growth kinetics is the one proposed by Andrews (Bailey & Ollis, 1986) which models the effect of substrate inhibition on microbial reproduction:

$$\mu(s) = \frac{s}{k + s + k_I s^2} \quad (2.)$$

According to Smith & Waltman (1995), the model in eq. (1) with a constant yield is not capable of explaining any oscillatory behaviour in a chemostat, independently of the kinetic expression chosen to describe the microbial growth. In the work by Pilyugin &

Waltman (2003), it is stated that a necessary condition to ensure the existence of dynamical regimes is to assume that the yield is not constant but dependent on the substrate concentration. A common assumption in literature to model periodic behaviour of a chemostat is to suppose a linear dependence of the yield coefficient on the substrate concentration (Agrawal et al., 1982). Therefore, it is assumed that:

$$y(s) = 1 + y_1 s \quad (3.)$$

A coefficient  $k_d$ , which takes account of the maintenance rate (van Bodegom, 2005), has been introduced in eq. (1): as reported in that paper, this term is included in the interval (0.01 - 0.1) in several experimental observations. In this work, an in-depth investigation about the existence and nature of the dynamical regimes for this type of reactor is performed: in particular, the analysis performed by Ajbar (2001) has been extended detecting all the sets of codimension one singularity for steady and Hopf points and plotting them in a non-persistent bifurcation diagram in the parameter plane spanned by  $k$  and  $k_f$ . This procedure allows obtaining information about the occurrence of global bifurcations. Furthermore, the effect produced by  $y_1$  on the occurrence of singularities is investigated.

## 2 Complete singularity diagram of a chemostat.

### 2.1 A list of the investigated singularity points

Before drawing the non-persistent bifurcation diagrams, a short explanation of the meaning of this instrument is appropriate: in a compact subset  $P$  of the parameter plane spanned by  $k$  and  $k_f$ , it is possible to plot some one-dimensional manifolds (e.g., curves) that determine the partition of  $P$  in some regions which show qualitatively similar solution diagrams of static and dynamical regimes as a function of the dilution rate. Unfortunately, this instrument is not problem-free. Golubitsky & Schaeffer (1985) reported a general theorem which states the topological equivalence for steady state solution diagrams belonging to the same region and also a weaker extension to the case of Hopf points, but no exhaustive conclusions can be drawn for periodic regimes or global bifurcations. However, despite this lack of generality about these complex behaviours, the singularity diagrams permit to obtain some interesting insights into them.

The static singularities, which occur in a chemostat with a kinetic law given by eq. (2) and a yield expression described by eq. (3), are:

1. Codimension one: transcritical (collision of two steady state branches with an exchange of respective stability properties).
2. Codimension two: pitchfork (a single stable (resp. unstable) steady state branch bifurcates into three steady state branches, two of them being stable (resp. unstable) and the third one unstable (resp. stable)).

The occurring dynamical singularities are:

1. Codimension one: Takens-Bodganov (TB) bifurcation (collision and annihilation of a Hopf and a homoclinic bifurcation on a saddle-node point), Hopf convergence or  $H_{01}$  singularity (collision of two

supercritical or two subcritical Hopf points), Bautin or  $H_{10}$  bifurcation (change from supercritical to subcritical type for a Hopf point or vice versa).

A third class of lines must be plotted in the singularity diagram: a limit to physically meaningful regimes on a solution diagram is that  $dil \geq 0$ ; therefore, the loci of transcritical, saddle-node or Hopf points occurring when  $dil=0$  are the ones that separate regions in which such bifurcations occur from the ones in which they have disappeared in the corresponding solution diagrams.

## 2.2 Singularity diagram for a chemostat with $y_1=10$ and $k_d=0.05$ .

The above listed loci are computed by deriving the Lyapunov-Schmidt reduction for both static and Hopf points and then determining the analytical equations that satisfy the degeneracy conditions for each type of singularity (Golubitsky & Schaeffer, 1985).

In figure 1, the singularity diagram for the case  $y_1=10$  and  $k_d=0.05$  is reported; in figure 2, the solution diagrams corresponding to the regions defined in figure 1 are plotted. These latter have been obtained using the continuation software AUTO2000 (Doedel et al., 2006).

A general description of the system can be given by comparing the dynamics of the resulting 13 regions. Zone 13, characterised by high values of both  $k$  and  $k_1$  which determine a very small  $\mu(s)$ , shows only washout solutions: in fact, these conditions prevent the population from growing because the maintenance term is greater than the growth process. The lines that delimit this subset are the threshold of minimum functionality of the bioreactor and, if the physical parameters lie over them, then the choice of substrate is inadequate or there are some other limiting factors that prevent the culture from growing in such a chemostat. Even the regions close to this border line are characterised by low productivities and steady solutions with low dilution rates; in fact the maximum growth rate can also be limited to 1% of the theoretical maximum growth rate (see plot 11 in figure 2).

As reported by Ajbar (2001), the equation of the pitchfork singularity line is  $k=k_1$ . If  $k > k_1$ , dynamical phenomena are quite unlikely: in fact, periodic behaviours for  $k > k_1$  occur only when the inhibition constant is very low (region 6). The black dashed line separates the regions in which the intersection of the nontrivial and the washout branch occurs from the ones in which they do not cross: in the latter case, the washout solution is always stable and the stable manifold of the intermediate unstable regime separates the basin of attraction of this point from the one corresponding to the nontrivial stationary point.

The behaviour of the system is much more interesting when  $k < k_1$ : under the pitchfork singularity line, a saddle-node bifurcation, essentially due to the presence of the maximum in the kinetic law, appears in the solution diagram. In this case the nonlinearities of the system have a stronger influence and this is proved by the appearance of dynamical solutions. In regions 3 and 8, periodic solutions originating from  $H_{01}$  singularity points are present. The two plots related to region 3 pinpoint a limit of the singularity approach: as can be observed, a single diagram is not sufficient to characterise the dynamical behaviour of this zone (i.e., it does not show all equivalent solution diagrams).

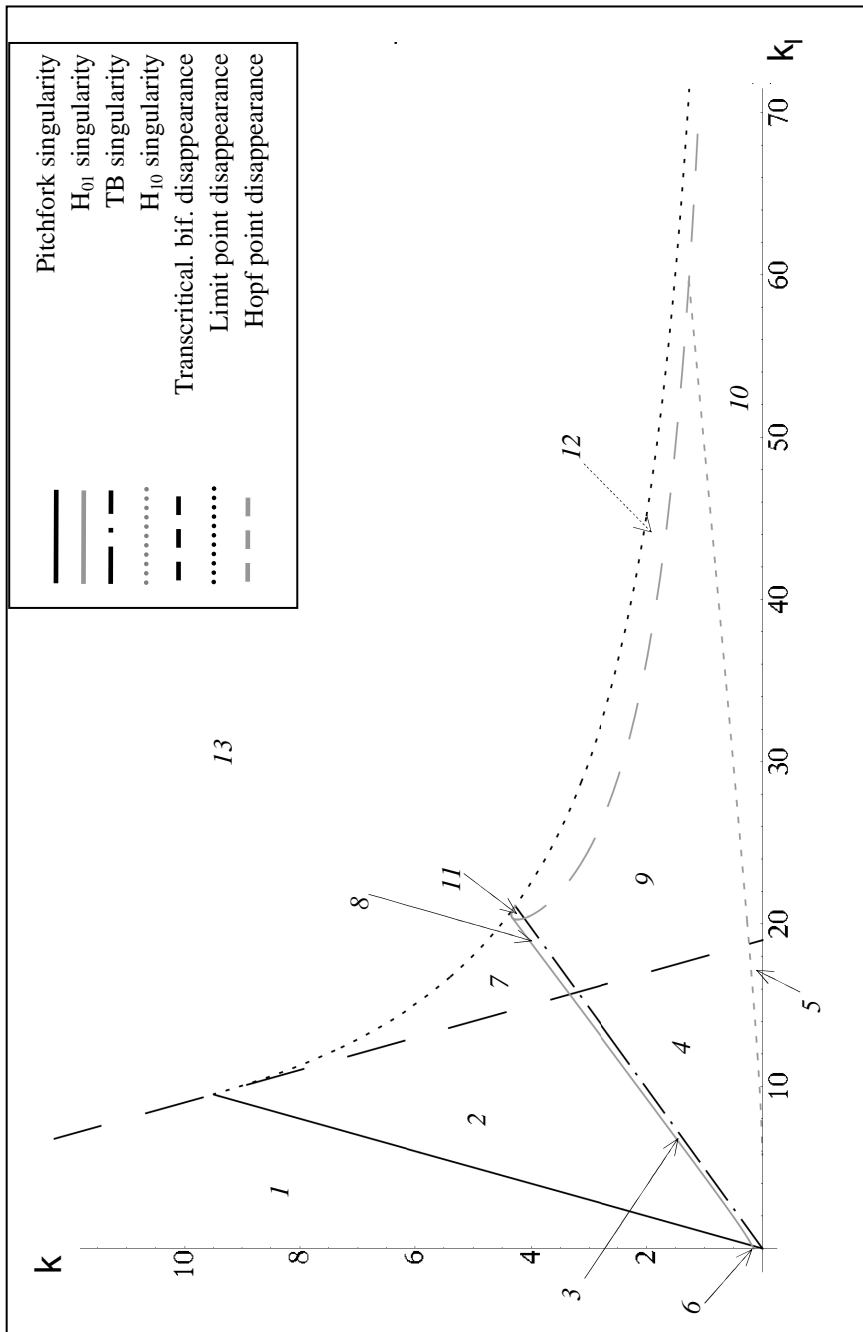
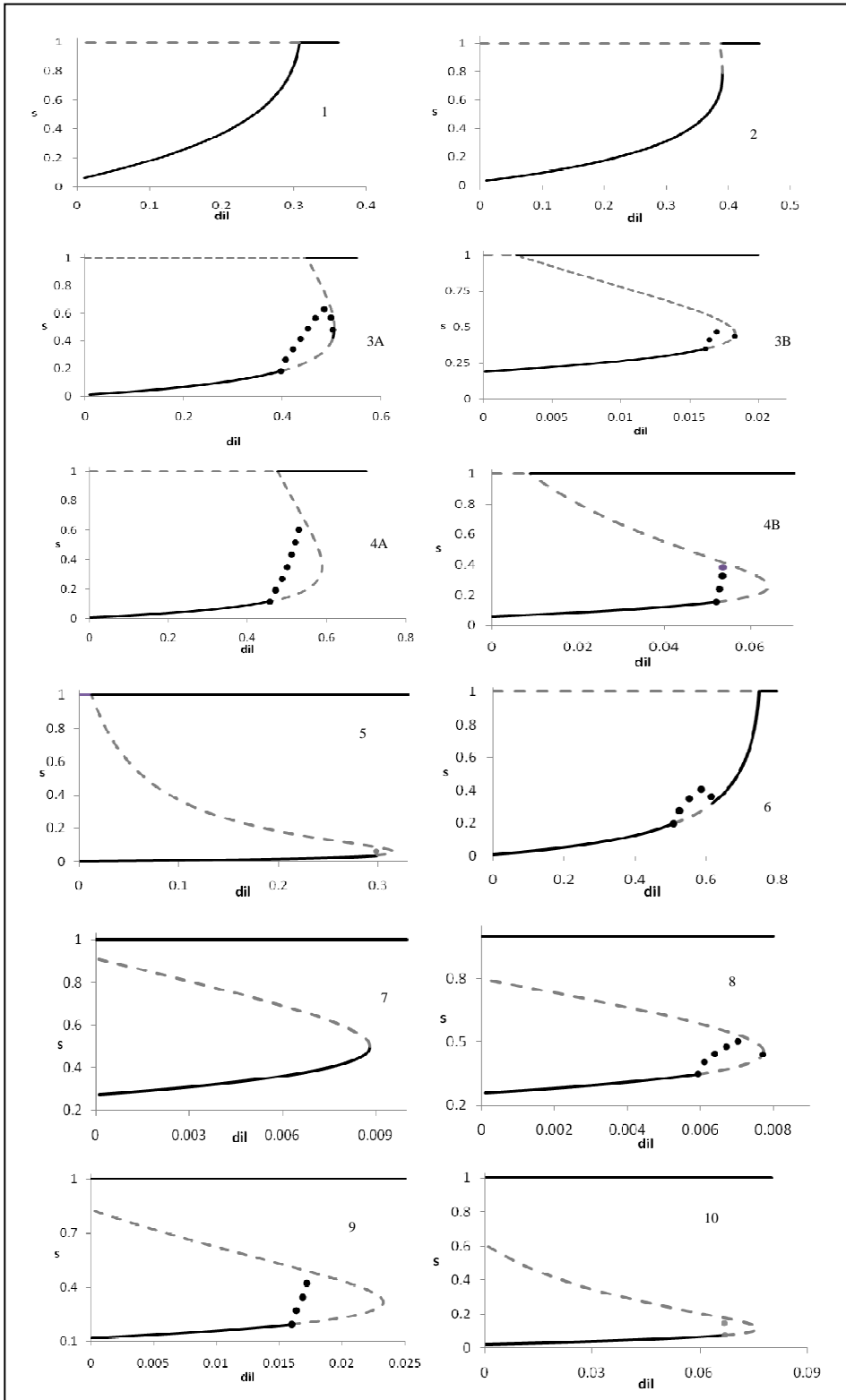


Figure 1: Singularity diagram for a chemostat with an Andrews growth kinetics and linear yield ( $y_1=10$ ,  $k_d=0.05$ ). Numbers are used to identify the regions in which the subset  $P$  of the 2D parameter subspace is partitioned.



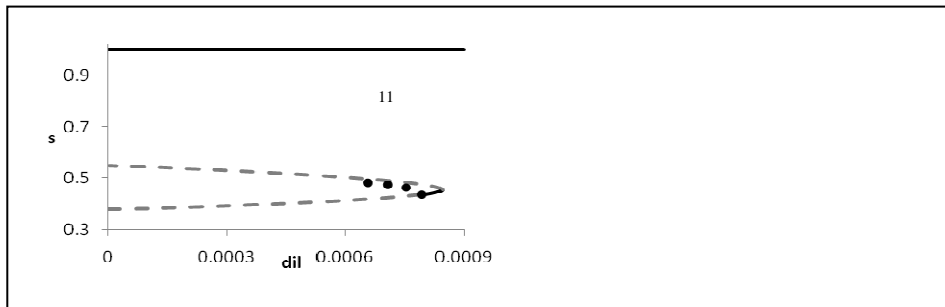


Figure 2 (on two pages): Solution diagrams for the regions defined in the previous figure 1.

In this case, the intersection of the stable periodic regime with the unstable steady state can cause the breakage of the periodic branch into two pieces terminating with a homoclinic bifurcation on the unstable steady branch: plot 3A shows the case in which a continuous periodic branch connects the two Hopf points, while plot 3B describes the case in which the global bifurcations appear: in the latter situation, the interval of dilution rates included between the ones in which homoclinic phenomena occur, is characterised by the absence of stable regimes except from the washout ones. Furthermore, region 8 has dynamical features similar to case 3B rather than 3A (with the only difference that the transcritical point does not appear in the solution diagram).

The dash-dot line indicates a TB singularity, that is, a collision between a Hopf point and the saddle-node (or limit) point. As defined before, a homoclinic bifurcation also converges in this point: this implies that, on the upper side of this line but close to it, the solution diagram must be similar to the one described in 3A of figure 2; in fact, this topology permits the collapse of the right Hopf point and the adjacent homoclinic bifurcation on the limit point when the dilution rate approaches the bifurcation value. In the lower part of the plot in figure 1, (that is, under the TB locus), only the left Hopf point and its correspondent homoclinic bifurcation survive as indicated by diagrams 4A, 4B and 9 in figure 2. Also in region 4 some global bifurcations occur and, hence, two non-equivalent solution diagrams are required to characterise it. In diagram 4A the periodic branch for the left Hopf is made up of only stable periodic orbits like the ones in region 3 while for high  $k_I$  and low  $k$  a fold bifurcation appears (starting from the homoclinic one) and some unstable limit orbits arise: in particular, the homoclinic bifurcation occurs between an unstable point and an unstable limit cycle for this subset of region 4 (see plot 4B). A similar phenomenon can be observed also in region 9.

The dotted gray line indicates the singularity locus in which the instability of the periodic orbits branch expands up to the Hopf point eliminating the stable ones: therefore both in region 5 and 10, the Hopf point is subcritical and no stable periodic orbits exist.

A final remark has to be made about the disappearance of Hopf points: the dashed gray line indicates the boundary for this type of singularity. In the part of parameter space

bordered by the  $H_{10}$  and the TB singularity, two Hopf points occur; in region 11 one of these points disappears while the second one vanishes when the right part of the curl line which encloses region 11 is crossed. As already said, under the TB singularity line a single Hopf point exists: this bifurcation point disappears when the dashed gray line is crossed: in this region all the steady points are unstable and the only stable regimes are periodic ones (as in region 12, for which the solution diagram is not reported here).

### 3 The effect of $y_1$ on the dynamics of the chemostat

A description about the effect of  $y_1$  on the singularity diagram follows. In order to evaluate its influence, the singularity diagrams for different values of these parameters are drawn.

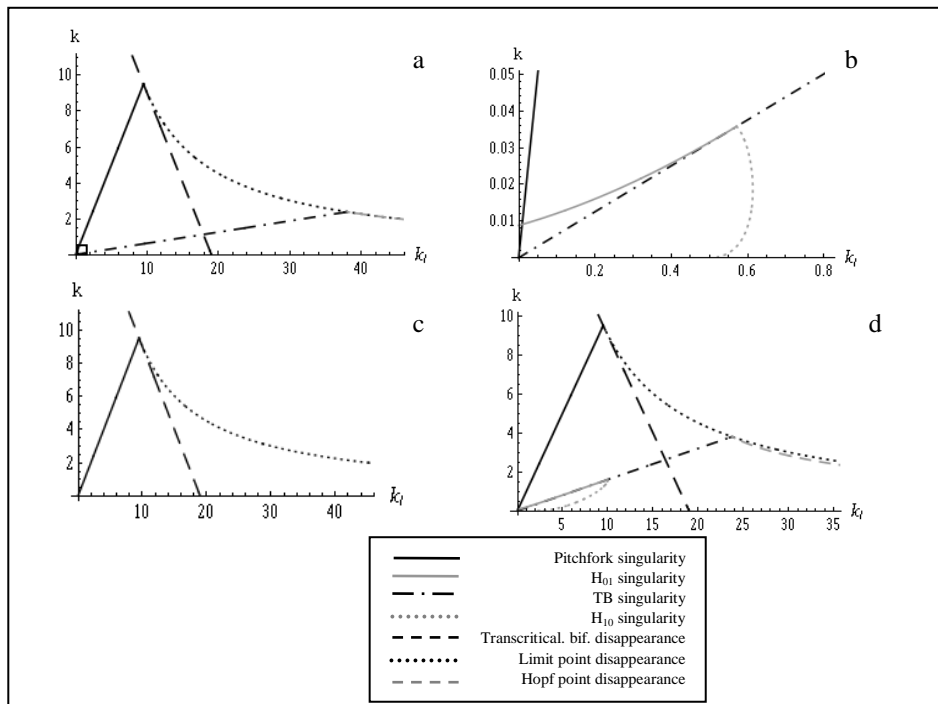


Figure 3: Singularity diagrams for  $k_d=0.05$ , (a)  $y_1=2$ , (b) magnification of the detail in the black square for case (a), (c)  $y_1=0.5$ , (d)  $y_1=5$ .

In agreement with the conclusions obtained by Ajbar (2001), only if  $y_1 > 1$  is it possible to observe dynamical regimes. Therefore, if  $y_1 < 1$ , the only singularity lines that are present in the diagram are the pitchfork and the disappearance ones (therefore only static singularity lines, as can be observed in figure 3c).

In figure 3a and b, the singularity diagram for  $y_1=2$  is reported. As can be seen, a first evident effect is the significant reduction of the region between the  $H_{01}$  and the TB singularity curves: differing from the previous case, the two lines cross each other

causing the interruption of the  $H_{01}$  curve in the intersection point that will be called S where also the  $H_{10}$  singularity curve converges; therefore the region with the presence of two Hopf points is much narrower than in the case  $y_1=10$  and the S point is a singularity with a higher codimension than one as there is a convergence of two codimension one curves in it. Similarly to figure 1, the region included between TB and  $H_{10}$  line shows solution diagrams with a single periodic branch and the closer the parameter point to Bautin curve is, the smaller the portion of periodic stable solutions around the Hopf point is in the corresponding solution diagram (this behaviour is similar to the ones in figure 2 case 4B): in fact, stable limit cycles disappear if the parameters belong to the region behind both the TB and the  $H_{10}$  curves (like the one plotted in figure 2 case 5). An obvious consequence of this observation is that from a TB point located on the left of S, the Hopf point collapsing on it is supercritical while it is subcritical if the TB point is positioned on the right of S in figure 3a and b.

Therefore it is possible to conclude that stable periodic regimes (which can be effectively observed) are possible only for parameter points lying in the area enclosed by the vertical axis, the  $H_{01}$  and the  $H_{10}$  singularity lines. Comparing figures 1, 3a, 3c and 3d, it can be deduced that decreasing the  $y_1$  value, the TB- $H_{01}$ - $H_{10}$  intersection singularity point moves progressively towards the origin up to vanishing for  $y_1=1$ ; hence, lowering  $y_1$  limits more and more the occurrence of stable periodic regimes (see, for example the case  $y_1=2$  plotted in figure 3b in which the region with stable limit cycles is very small); on the contrary when the parameter increases, the TB- $H_{01}$ - $H_{10}$  intersection moves towards the disappearance loci until it vanishes. At this point, it generates the curl of the dashed gray curve, which encloses region 11 in figure 1 and indicates a different disappearance mechanism for the two Hopf points.

## 4 Conclusions

A final summary about the dynamics of the chemostat is that the effect due to the positive slope of the yield function with substrate concentration is the main cause of oscillating regimes; unstable periodic regimes are possible as well as subcritical Hopf points (that Ajbar, 2001, did not indicate) as the inhibitive action becomes stronger; instead, the occurrence of stable periodic regimes is more likely for rapidly growing yields and low inhibition constant.

## 5 References

- Agrawal, P., Lee C., Lim, H. C., Ramkrishna, D., 1982, Chem. Eng. Sci. 37, 453  
Ajbar, A., 2001., Chem. Eng. Sci. 56, 1991.  
Bailey G.E., Ollis D.F, 1986 Biochemical Engineering Fundamentals. MacGraw Hill.  
Doedel E.J. et al. 2006, Auto 2000. <http://sorceforgne.net/projects/auto2000>.  
Golubitsky M. & Schaeffer A., 1985., Singularities and groups in bifurcation theory. Springer Verlag  
Kuznetsov, Y.A., 2000, Elements of Applied Bifurcation Theory. Springer, New York.  
Pilyugin S.S.- Waltman P., 2003, Mathematical Biosciences. 182, 151-166.  
Smith M. & Waltman P., 1995, The theory of the chemostat. Cambridge Univ. Press.  
Van Bodegom P., 2007., Microbial ecology. 53, 513.